Experimental Investigations on the Crystallization of Zinc by Direct Irradiation of Zinc Oxide in a Solar Furnace

A. Weidenkaff,* A. Reller, F. Sibieude,† A. Wokaun,‡ and A. Steinfeld§

Inst. Solid State Chemistry, University of Augsburg, Universitätsstr. 1, D-86159 Augsburg, Germany, CNRS−IMP, Bp-5 Odeillo, F-66125 Font-Romeu Cedex, France, Department General Energy Research, Paul Scherrer Institute, CH-5232 Villigen, Switzerland, and Department of Mechanical and Process Engineering, ETH-Swiss Federal Institute of Technology, CH-8092 Zurich, Switzerland

Received March 2, 2000. Revised Manuscript Received April 7, 2000

Concentrated solar irradiation was used to thermally dissociate ZnO and to study the zinc vapor condensation process in the presence of oxygen under several dilution, temperature, pressure, and irradiation conditions. Product samples were taken from targets on the condenser surface and were analyzed with X-ray diffractometry and scanning electron microscopy. The zinc oxide formation by reoxidation of zinc was found to be of a heterogeneous nature, with homogeneously condensed zinc serving as the main nucleation sites. High zinc yields were obtained under conditions which favor supersaturation of zinc vapor and high deposition rates of zinc, whereby separation of condensing zinc and oxygen is desired.

Introduction

The thermal conversion of solar energy into chemical fuels, "solar fuels", offers the possibility of efficiently storing and transporting solar energy. By concentrating the sunlight with the help of parabolic mirrors, we can provide high-temperature solar process heat for driving endothermic processes. One possibility has been demonstrated by the solar thermal reduction of oxidized transition metal oxides (e.g. Fe_3O_4 or ZnO). The corresponding products, which are either metals (e.g. Zn) or lower valenced metal oxides (e.g. FeO) can be used to split water for producing hydrogen as an environmentally neutral fuel. The identification of efficient and technically feasible thermochemical cycles requires detailed studies on both the reduction and reoxidation step. Among the studied candidate systems functioning within an accessible temperature range, zinc oxide (ZnO) is the most promising.

The reaction proceeds fast enough near 2000 K, yielding metallic zinc and oxygen. Zinc is a versatile metal: besides being a widely used commodity in the galvanizing and chemical industries, it is also a compact and safe-to-handle solid fuel that finds applications in zinc/air fuel cells and in zinc/air batteries. In these devices zinc is oxidized to produce electricity. Zinc can also be reacted with water to form hydrogen that can be further processed for heat and electricity generation.[1] Such a two-step water-splitting cycle is represented by

$$ZnO \rightleftharpoons Zn(g) + 0.5O_2 \qquad \text{(first solar step, endothermic)}$$

$$Zn + H_2O \rightleftharpoons ZnO + H_2 \qquad \text{(second step, exothermic)}$$

The chemical thermodynamics and kinetics of reactions (1) have been reported in previous publications.[2,3] The most important results are briefly reviewed.

The equilibrium mole fractions of Zn(g) and O_2 are 0.67 and 0.33, respectively, in the temperature range between 1700 and 2400 K.[2] The reaction enthalpy is $\Delta H_{298K} = 348$ kJ/mol. The decomposition rate of ZnO(s) was measured by thermogravimetry in a N_2 atmosphere; the apparent activation energy obtained was 312 kJ/mol, which is similar to a value cited in ref 4. The product gases need to be quenched to avoid reoxidation but the efficiency of the quench is sensitive to the dilution ratio of zinc and oxygen in the gas flow and the temperature of the surface on which the products are quenched. The condensation of Zn(g) in the presence of O_2 was studied by fractional crystallization in a temperature-gradient tube furnace. The oxidation of Zn is a heterogeneous process, and in the absence of nucleation sites, Zn(g) and O_2 can coexist in a metastable state. However, as soon as zinc condenses, reoxidation can occur.

An understanding of the parameters that favor the formation of pure zinc is required. The present paper is concerned with the effect of the condensation condi-

* Corresponding author. Tel.: (49) 821 598 3270. E-mail: anke.weidenkaff@physik.uni-augsburg.de.
† CNRS-IMP.
‡ Paul Scherrer Institute.
§ ETH-Swiss Federal Institute of Technology.

(1) Bilgen, E.; Ducarroir, M.; Foex, M.; Sibieude, F.; Trombe, F. Use of solar energy for direct and two-step water decomposition cycles. *Int. J. Hydrogen Energy* **1977**, *2*, 251−257.
(2) Palumbo, R.; Lédé, J.; Boutin, O.; et al. *Chem. Eng. Sci.* **1998**, *53*, 2503−2518.
(3) Weidenkaff, A.; Steinfeld, A.; Wokaun, A.; Auer, P. O.; Eichler, B.; Reller, A. *Solar Energy* **1999**, *65*, 59−69.
(4) Hirschwald, W.; Stolze, F. *Zeitschr. Phys. Chem.* **1972**, *77*, 21−42.

10.1021/cm0010295 CCC: $19.00
Published on Web 07/13/2000

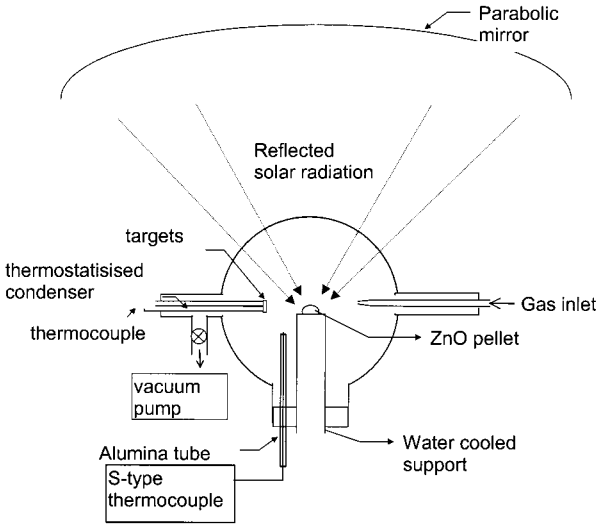

Figure 1. Schematic of experimental setup for the solar thermal dissociation of ZnO.

tions on the zinc yields during the solar thermal dissociation of ZnO.

Experimental Section

The experiments were conducted in the 2 kW solar furnace in Odeillo, France. The vertical axis solar concentrating system consists of a sun-tracking heliostat and a 2 m diameter parabolic concentrator capable of reaching a peak energy concentration of 1600 W/cm^2.[5]

The solar chemical reactor scheme shown in Figure 1 consists of a water-cooled copper sample holder enclosed by a Pyrex dome positioned at the focus of the solar furnace. With this arrangement the reactants are directly illuminated by the high-flux solar radiation focused on a 8 mm diameter circular spot.

The samples were prepared as 10 mm diameter pellets of pressed pure ZnO (Aldrich Nr. 14439), technical ZnO, and powder mixtures of ZnO with other inert metal oxides (e.g. 60−80% ZrO_2, Y_2O_3, or Er_2O_3).

Previous to each experiment, the Pyrex dome was evacuated and then filled with argon. The energy input was controlled by opening the shutter to different positions (between 60 and 100%) or by varying the position of the sample holder in the solar furnace's *z*-axis. The temperatures and heating rates achieved during irradiation were estimated by melting ceramic materials of high melting points, to give the following: powder of erbium oxide (Er_2O_3, mp = 2400 °C), zirconium oxide (ZrO_2, mp = 2700 °C), or yttrium oxide (Y_2O_3, mp = 2430 °C).[6] The heating rates were typically in the range of 1000 °C/s.

The pellets were illuminated for various exposure time periods. The gaseous products, zinc and oxygen, evolved from the surface of the ZnO pellet and were transported by a flow of inert gas and by applying vacuum pressures downstream. The condensable products (Zn and ZnO) were collected simultaneously on six targets of 1 cm^2 each, located at the condenser (front side and laterally). The amount of dissociated ZnO was determined after the experiment. The following experimental parameters have been varied during the experiments: the pressure inside the Pyrex dome was varied from 10 mbar to atmospheric pressure by changing the capacity of the vacuum pump and the gas flow rates; the argon gas flow rate was varied from 0 to 9 L/min; the distance between the dissociating sample and the condenser was varied from 3 to 25 mm; the temperature of the condenser surface was varied between 6 and 30 °C; the sample illumination time (t_{illu}) was varied from 1 to 120 s. The composition of the parent pellet was either pure ZnO, technical (impure) ZnO, or ZnO mixtures with ZrO_2, ErO_2, or Y_2O_3).

Results and Discussion

To elucidate the different stages and forms of nucleation, crystal growth, and reoxidation, the condensed products collected from the targets were examined after each solar experiment by scanning electron microscopy (SEM) and by X-ray diffractometry (XRD). The zinc yield in the deposit defined as molar zinc fraction of Zn in ZnO has been determined semiquantatively by powder X-ray diffraction (with an accuracy of ±7%[7]). The influence of parameters such as gas flow rate, pressure, temperature, and surface properties of the implemented nucleation sites on the product morphologies has been studied for several experiments. Depending on the experimental conditions, the zinc yield in the products varies between 3 and 99% Zn in ZnO. The dissociation rate varies between 0.7 and 135 mg/s.

4.1. The Gas Phase. In the solar furnace, the irradiation of ZnO pellets leads to the formation of gaseous zinc and oxygen. From literature it is known that gaseous ZnO only exists as highly activated species with an extremely short lifetime.[8,9] Thus, under the given experimental conditions, the existence of gaseous ZnO can be excluded. During the actual experiments, zinc vapor and oxygen evolving from the ZnO pellet are diluted by the argon flow until phase transitions occur, either through the condensation and/or desublimation of zinc or through the formation of solid zinc oxide by reoxidation processes. As a consequence, the partial pressures of zinc and oxygen decrease while the amount of inert gas remains constant. The steady-state partial pressure of gaseous zinc depends on the argon flow rate and the ZnO dissociation rate. During start-up and shut-down periods of the experiment, the composition of the gas phase is affected by transients due to heating/cooling and filling of the evacuated space inside the Pyrex dome.

Immediately after the shutter of the solar furnace system is opened and the ZnO pellet is irradiated, a vigorous reaction is observed. The formation of gaseous zinc and oxygen by the dissociative sublimation of ZnO leads to a pronounced increase of the local pressures: In several experiments, the pellets were even moved out of the focal position; these experiments had to be interrupted and could not be evaluated. The rate of the ZnO dissociation depends directly on the heating rate, which in turn depends on the solar irradiation, and the properties of the ZnO pellet, namely its absorptivity, size, density, and thickness. Due to the fact that the focal area is in the range of the dimensions of the pellets, these have to be moved along the *z*-axis in order to adjust a constant irradiation diameter.

During the experiments, product deposition takes place on the surface of the Pyrex dome. This leads to a more or less pronounced decrease of the pellet illumina-

(5) Ambriz, J. J.; Ducarroir, M.; Sibieude, F. *Int. J. Hydrogen Energy* **1982**, *7*, 143−153.
(6) Stubican, V.; Ray, S. *J. Am. Ceram. Soc.* **1977**, *11*, 534.
(7) Widmer, P.; Estermann, A. *Ermittlung und Eichung einer Methode zur schnellen Bestimmung des Zinkgehaltes in Zn/ZnO-Mischungen. Semesterarbeit.* Paul Scherrer Institut, CH: Villigen, Switzerland, 1997.
(8) Chertihin, G. V.; Andrews, L. *J. Chem. Phys.* **1997**, *106*, 3457−3465.
(9) Liu, Z.; Gelinas, M. P.; Coombe, R. D. *J. Appl. Phys.* **1994**, *75*, 3098−3104.

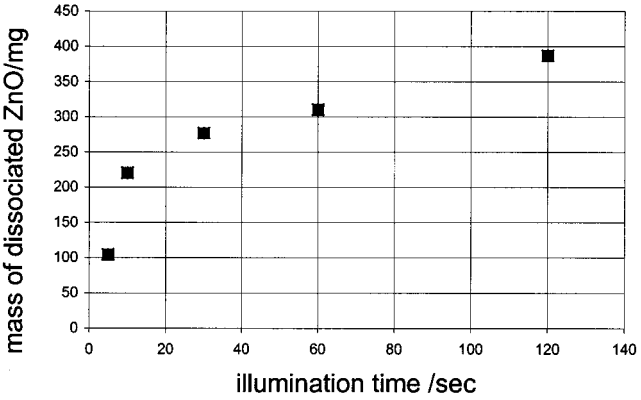

Figure 2. Mass of ZnO dissociated in experiments with different illumination periods, performed at 0.03 bar with 2 L/min Ar flow.

tion and, consequently, the dissociation rate of ZnO. During the first 30 s of illumination (at experimental pressures lower than 0.2 bar), the reaction rate is only slightly decreased by the mentioned product deposition leading to partial shading of the sample. Accordingly, longer periods of pellet illumination result in a remarkable decrease of the pellet temperature and the dissociation rate (see Figure 2).

Presintering of the parent pellet and/or sintering effects during the solar experiments lower the dissociation rate. This result can be explained by a smaller reaction area from which gas desorption can take place. SEM images of partly dissociated ZnO pellets after the experiment show a rough surface with many concavities due to material ejection.

For pellets containing mixtures made up of ZnO and inert metal oxides such as alumina, silica, yttria, erbia, and zirconia, we noticed a delayed beginning of the dissociation. The comparison between different ZnO/inert metal oxide ratios indicates, however, that higher dissociation rates can be obtained. Evaluation of different experiments confirms an increase up to 20%. For example, the heating of a pellet made up of an initial compound mixture of 74 mol % ZnO in Y_2O_3 leads to the dissociation of 477 mg of ZnO in 30 s, whereas only 387 mg of ZnO is dissociated in 30 s starting from a pellet of pure ZnO.

The higher dissociation rates for the oxide mixtures is attributed to the higher rates of convection heat transfer through the melt in addition to the radiation absorption. For similar metal oxide melts, temperatures in the range of 2700 °C have been registered.[1] This is far above the temperature for which ZnO(s) is stable, resulting in overheating of the material.

SEM images of the molten and resolidified pellets reveal a highly textured surface (see Figure 3), suggesting that either the viscosity of the melt was low or the solidification rate was high.

The pressure in the reactor and the inert gas flow rate determine the mass transport of the products and thus the local equilibrium on the ZnO surface.

In comparative experiments we investigated the influence of the argon flow rate on the product formation. Higher inert gas flows induce higher dissociation rates due to a faster product transport. For instance, in experiments 8−11 the dissociation rate of ZnO changes from 3.9 mg/s when no argon flow is applied to

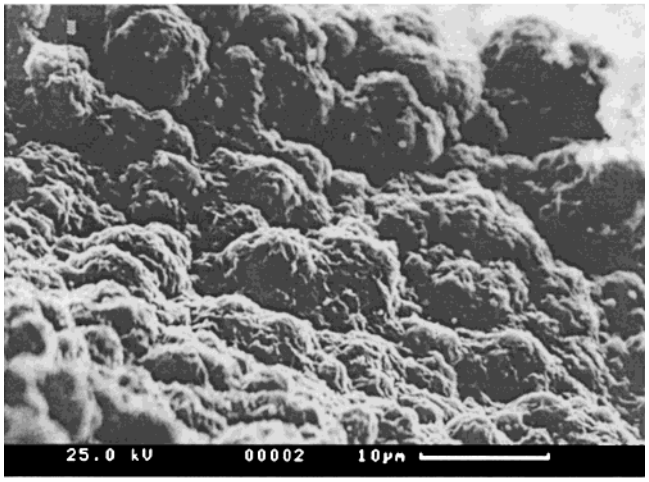

Figure 3. Scanning electron micrograph of highly textured surface of ZnO/ZrO_2 pellet after a 5 s illumination period.

9.2 mg/s for a 4.3 L/min argon flow. The resulting higher partial pressure of zinc is diluted by the higher amount of argon. The highest zinc yield is obtained for a gas flow rate of 2.9 L/min.

The pressure inside the Pyrex dome influences the ZnO dissociation rate and the zinc yield in the products. In experiments at lower pressure (p < 0.013 bar), up to 45% more ZnO dissociates because of the faster removal of products from the ZnO surface. The zinc yields at lower pressures are generally higher than at elevated pressure, as observed in experiments 8 and 5. The product obtained at 0.13 bar contains 59% Zn, whereas the product obtained at 0.4 bar under the same conditions yields only 13% Zn.

In comparison with other experiments, more shading (caused byproduct deposition on the Pyrex dome) was observed at ambient pressure than at lower pressures. At elevated pressures the products are scattered into all directions, whereas at low pressures the products are transported directly to the condenser.

At ambient pressure it was observed that after the first second, a part of the product was already deposited on the surface of the Pyrex dome. The resulting shading effect leads to a pronounced decrease of the ZnO dissociation rate and consequently to the zinc deposition rate toward the end of comparatively long experiments. For short experiments, e.g. an experiment of 1 s illumination time at ambient pressure, a zinc yield of 71% results. A possible explication for this remarkable difference in the zinc yield is that the experiments differ in the product deposition rate.

After the experiments, the residues of the parent pellets at ambient pressure and at 0.4 bar are covered with zinc oxide needles formed by the recombination of zinc and oxygen directly on the pellet surface. A higher yield of a tetrapod like ZnO (T-ZnO) was observed at higher pressures (see the following section).

4.2. The Condensed Phase. Condensed product samples collected on the condenser surface were analyzed by XRD. In all experiments metallic zinc was detected. Usually, yields in the range of 40−70 mol % zinc in zinc oxide were found. Exceptions were found for experiments conducted in air: A high excess of the oxygen partial pressure in the system results in a nearly

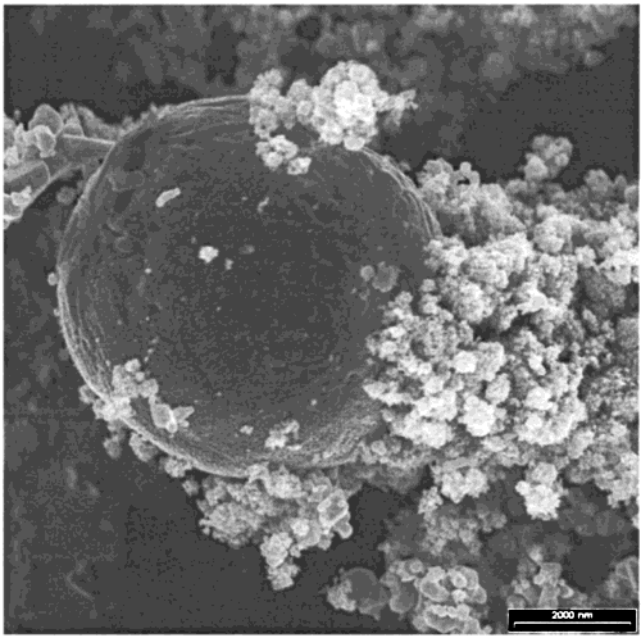

Figure 4. Scanning electron micrograph of condensed product from ZnO dissociation: Typical product morphology shows relatively large zinc droplets and fine material.

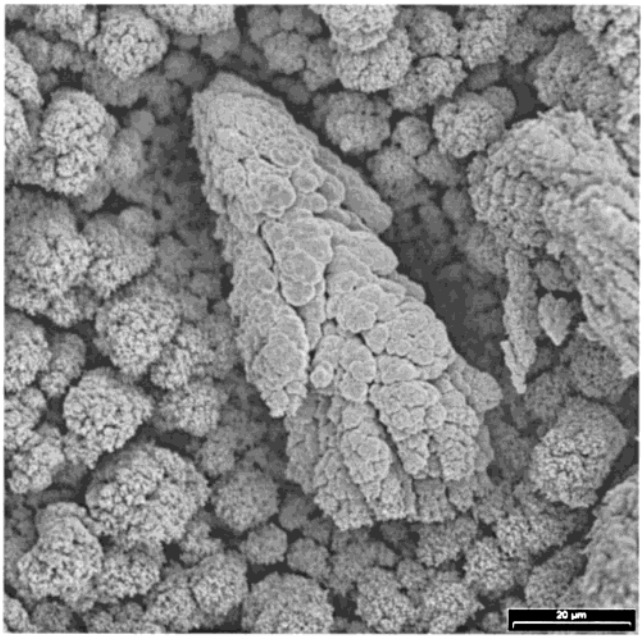

Figure 5. Scanning electron micrograph of condensed product from the water-cooled target surface obtained in ZnO dissociation. Small particles and large dendritic intergrown crystallites are found.

complete product oxidation. This indicates the necessity of oxygen dilution or removal during the experiment.

The highest zinc yields were obtained from short experiments (t_{illu} < 10 s) with very high dissociation rates (ζ > 100 mg/s). It was previously observed by Bilgen et al.[1] and confirmed by our experiments that the zinc yield in the condensed phase can be higher when zinc oxide is heated in a matrix of zirconia, yttria, or erbia. Morphological studies reveal relatively large zinc droplets and—in a subsequent step—finely dispersed ZnO (see Figure 4).

The amount of nucleation sites seems to vary from experiment to experiment. Products made up of many small particles and large dendritic intergrown crystallites (see Figure 5) are detected. In most cases both extremes are found on the same target.

The growth mechanisms of zinc and zinc oxide suggested in this paper (see below) are based on detailed morphological products analysis. Scanning electron micrographs of the grown crystals reveal a very heterogeneous morphology. The particle size of the products is in the range of few nanometers to several micrometers in diameter. SEM images reveal a mixture of compact, coarse, dropletlike (see Figures 4 and 7), and filigran particles (see Figure 6a,b). The particle surface can be rough, topped with ZnO, or smooth.

The formation of dropletlike particles found on the target surface (see Figures 4 and 7) suggests that the material was liquid before solidification and that either the condensation takes place before reaching the condenser surface (homogeneous nucleation) or "island growth" (heterogeneous nucleation) occurs.

This heterogeneous but three-dimensional growth mode is known as the Vollmer–Weber growth mode[10] and is observed when the interfacial energy between the substrate and the deposit (adhesion) is lower than the energy between the atoms of the condensate (cohesion). In our experiments, the adhesion of the condensed phase on the target surface is very low; therefore, both mechanisms are possible.

Samples taken from the front side of the condenser or from sites neighboring the illumination spot, where the vapor temperature and the zinc vapor pressure are high, contain more deposit with bigger particles of up to 10 μm diameter. On the targets located laterally on the condenser, less product was deposited because most of the zinc vapor was already removed from the gas stream by condensation. These particles are fine (~100 nm), due to the high nucleation rate at a low growth rate. This can be explained by the lower mass transport of zinc. Similar observations were made previously for solar experiments.[11]

The dropletlike particles are most probably condensed zinc, which is also supported by energy-dispersive X-ray spectroscopy (EDX). Under the given conditions, zinc oxide cannot form a liquid phase during solidification.

Generally, ZnO can be found in the form of crystalline whiskers.[12] The whisker length depends on the process parameters and can vary from nanometers to attain several millimeters (see Figure 6).

The morphology of ZnO particles obtained in experiments with a very low zinc partial pressure or when most of the zinc is already condensed shows the characteristic tetrapod shape, so-called T-ZnO, with platelets bridging between legs (see Figure 6b). They resemble the morphology reported in refs 13 and 14 and their growth mechanism on an inserted zinc nucleus is

(10) Gilmer, G. H.; Grabow, M. H. *JOM* **1987**, *39*, 19–23.

(11) Steinfeld, A.; Brack, M.; Meier, A.; Weidenkaff, A.; Wuillemin, D. *Energy* **1998**, *23*, 803–814.

(12) Ataev, B. M.; Kamilov, I. K.; Mamedov, V. V. *Technol. Phys. Lett.* **1997**, *23*, 842–843.

(13) Kitano, M.; Hamabe, T.; Maeda, S. *J. Cryst. Growth* **1990**, *102*, 965–973.

(14) Kitano, M.; Hamabe, T.; Maeda, S. *J. Cryst. Growth* **1991**, *108*, 277–284.

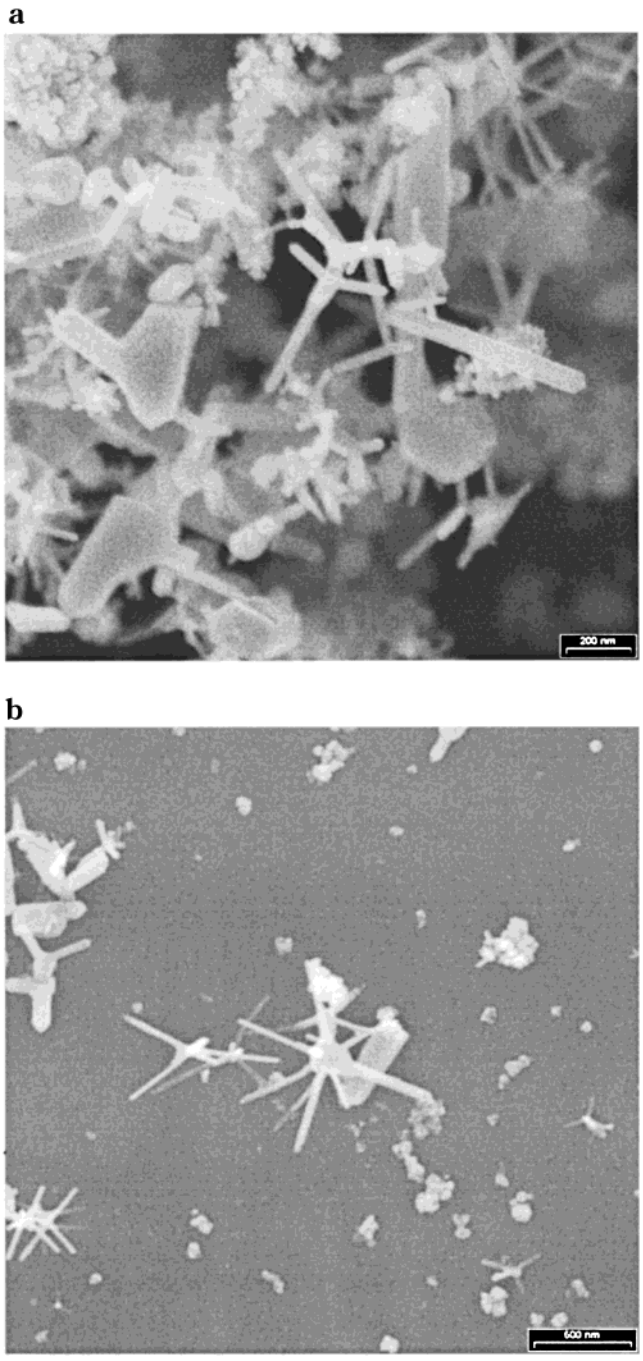

Figure 6. Scanning electron micrograph of condensed product on the water-cooled target: fine material with tetrapod-shaped ZnO (a) and tetrapod-shaped ZnO with dropletlike nuclei (b).

discussed in refs 14−19. Transmission electron microscopy of the T-ZnO particles shows differences between the structural features of the center and the leg crystals, similar to the samples obtained previously.[16] The legs crystallize in a wurtzite structure with the *c*-axis parallel to the leg-axis. The nucleus has a different crystallographic structure than the leg crystals, but a

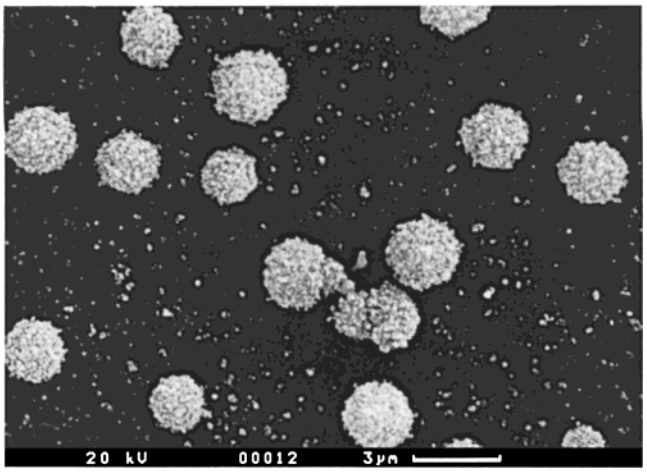

Figure 7. Scanning electron micrograph of condensed product on the water-cooled target surface shows spherical structures with a rough surface.

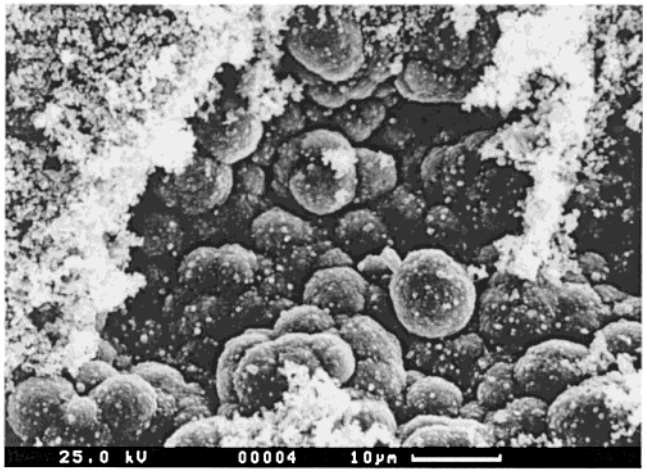

Figure 8. SEM image of the deposit on the pellet surface 1 mm next to the illuminated spot.

detailed identification was not possible because of its small size (few nanometers). Such structural differences may be due to condensed zinc forming at the very initial stage of T-ZnO crystallization.

Products found on hot parts of the apparatus (e.g. gas inlet, pellet surface) mostly contain high yields of zinc. SEM images of the pellet surface 1 mm next to the illuminated spot show deposited zinc droplets and fine ZnO particles (see Figure 8). The zinc partial pressure directly over the pellet must have been relatively high, especially when the transport velocity and the dilution are low.

The partial pressure of oxygen, the deposition rate, and the gas temperature are not likely homogeneous throughout the Pyrex dome. The Pyrex itself is also not uniformly irradiated. We observed a black and adhesive layer, with a zinc content of more than 60%, formed at the top of the Pyrex dome. The rest of the Pyrex surface was covered with a white material, not sticking to the surface, which consisted of fine ZnO needles.

This dramatic difference of product formation has also been observed previously in thermochromatographic studies.[3]

4.3. Processes during Trajectory and Deposition. During the trajectory of the volatile species from the dissociation site (the illuminated spot) to the deposition

(15) Fujii, M.; Iwanaga, H.; Ichihara, M.; Takeuchi, S. *J. Cryst. Growth* **1993**, *128*, 1095−1098.
(16) Iwanaga, H.; Fujii, M.; Ichihara, M.; Takeuchi, S. *J. Cryst. Growth* **1994**, *141*, 234−238.
(17) Iwanaga, H.; Fujii, M.; Takeuchi, S. *J. Cryst. Growth* **1998**, *183*, 190−195.
(18) Iwanaga, H.; Shibata, N. *J. Cryst. Growth* **1976**, *35*, 159−164.
(19) Iwanaga, H.; Yamaguchi, T.; Shibata, N. *J. Cryst. Growth* **1978**, *43*, 71−76.

site (the condenser surface or Pyrex surface), processes that are decisive to the product formation occur. The fundamental question is whether homogeneous or heterogeneous condensation processes decide upon the properties of the products. The observation of black smoke is a strong argument for the homogeneous nucleation of zinc in the initial stage of the trajectory. The dropletlike shape of condensed zinc corroborates this mechanism. If a heterogeneous condensation mechanism would occur, the different target surfaces and their temperatures would influence the product morphology. In our experiments, changing either the temperature (from 6 to 30 °C), the roughness, or type of the condenser (Cu, glass, or ZnO monocrystals) did not influence the product formation. Even varying the "time-of-flight" by decreasing the distance from the dissociation site to the condenser (from 25 to 1 mm) did not result in a visible change in the product morphology or zinc yield (see experiments 20 and 21). The temperature of the gas phase, measured 2 cm away from the illuminated spot, was 70 °C during the experiment. Thus, the products are cooled below the condensation temperature of zinc (~700 °C) before reaching the condenser.

The driving force for a phase transformation is the difference of the chemical potential of the corresponding phases. A vapor−liquid transformation is driven by the chemical potential difference

$$\Delta\mu = \mu_v(p,T) - \mu_l(p,T) \quad (1)$$

where μ_v is the chemical potential of the vapor and μ_l the chemical potential of the liquid phase. Zinc agglomerates to form liquid zinc at a critical saturation of zinc vapor. The temperature dependence of the zinc partial pressure is given by the following equation[20]

$$\log p_{Zn} = -6163/T + 8.108 \quad (2)$$

The formation of nucleation sites depends on the temperature, the zinc partial pressure, and the total pressure. The process of the initial nucleation includes collision of atoms, ordered grouping of atoms in the gas phase, formation of clusters and aggregates, formation of critical nuclei, and growth of these nuclei to a critical size. The hindrance of nucleus formation is due to the large specific surface area of the small droplets, which causes an increase of the vapor pressure on small aggregates.

The nuclei are formed at a critical supersaturation, achieved by cooling the zinc vapor (see eq 2). But very small zinc droplets can re-evaporate completely instead of growing. Impurities and reactor walls can lower the surface tension and act as nucleation sites.

The number of nuclei appearing in a unit of volume in a period of time depends strongly on the critical supersaturation, corresponding to the growth zone temperature. A small number of nucleation sites and fast growth of the new phase led to relatively large particles. We observed in thermochromatographic experiments[3] that a very high zinc vapor pressure leads to immediate and fast condensation at certain temperatures, resulting in relatively large droplets. It also needs to be considered that zinc which is already deposited may re-evaporate once the surface temperature of the deposition site exceeds the zinc evaporation temperature.

When the nuclei achieve a critical size, their further growth reduces the system energy (see eq 1) so that the condensation proceeds very fast. The growth velocity depends on the velocity of zinc transport to the new phase boundary.

Compared to a solid surface, a liquid surface is atomistically extremely rough and therefore a preferred site for deposition. At lower pressure the surface of the droplets is even more rough and larger than at ambient pressure.[21] This kind of surface provides many sites for adsorption; furthermore, zinc grows fast on liquid zinc. At temperatures lower than the condensation temperature, zinc can be deposited in two ways: (1) as a liquid layer on the already condensed phase (classical condensation) or (2) as a solid layer when the temperature is lower than the zinc melting point (desublimation).[3]

At temperatures lower than the melting point of zinc, a liquid−solid interface is formed and a vapor−liquid−solid (VLS) growth mode results.[22]

Assuming that a homogeneous nucleation process is taking place in our experimental runs, the cooling rate of the liquid zinc depends on the size of the droplets/particles during their transport from the illuminated spot to the condenser surface. Latent heat of crystallization is released in all directions. A fast cooling hinders the reverse, reoxidation reaction. The best conditions to grow products with high zinc yield are observed when the growth of zinc is faster than the growth of zinc oxide.

The oxidation of solid zinc is very slow because a layer of oxide on the surface inhibits the oxidation of bulk zinc by forming a protective skin, due to the higher molecular volume of the oxide.[23−25] The oxidation process is controlled by diffusion of zinc through the ZnO surface layer.[26]

ZnO whiskers are growing on wrinkles of the droplet surfaces. The latent heat of ZnO crystallization is released through the substrate.

To lower the ZnO formation rate, the rate-limiting factors need to be determined. Previous studies[27] assumed a reoxidation mechanism based on the diffusion of metal from the center of a particle through the metal oxide layer to the surface, where the metal eventually reacts with oxygen to form a new metal oxide layer. This reoxidation mechanism is not valid for the present chemical system because the source of zinc for the formation of ZnO is coming from the vapor phase.

(20) Knacke, O.; Kubaschewski, O. In *Thermochemical Properties of Inorganic Substances*l Springer-Verlag: Berlin, 1991; Vol. 2, pp 2336−2348.

(21) Yumoto, H.; Yoshihiko, G.; Naohiro, I. *Materials Transactions, JIM* **1989**, *30*, 741−747.

(22) Hasiguti, R. R.; Yumoto, H.; Kuriyama, Y. *J. Cryst. Growth* **1981**, *52*, 135−140.

(23) Guppy, A.; Wickens, A. J.; Fray, D. J. *Trans. Inst. Mining Metallurgy* **1972**, *81*, C236−C242.

(24) Zhang, X. *Corrosion and Elektrochemistry of Zinc*; Plenum Press: New York, 1996.

(25) Thomas, D. G. *J. Phys. Chem. Solids* **1957**, *3*, 229−237.

(26) Cope, J. O. *Trans. Faraday Soc.* **1961**, *57*, 493−503.

(27) Kitano, M.; Hamabe, T.; Maeda, S. *J. Cryst. Growth* **1993**, *128*, 1099−1103.

Conclusions

We have conducted a set of experiments in a high-flux solar furnace to study the formation of zinc by thermal dissociation of ZnO. The influence of the zinc vapor and oxygen dilution in inert gas during the experiment is complex. Experiments with low zinc vapor pressure (i.e. high dilution ratio) resulted in a slow growth of droplets and the formation of small particles with large specific surface areas which serve as nucleation sites and favor ZnO formation. Experiments with high zinc partial pressures (i.e. low dilution ratio) showed higher zinc content in the condensed phase than experiments with low zinc partial pressures, caused by faster growth of zinc and/or by the formation of larger particles with smaller specific surfaces areas. Evidently, the amount of nucleation sites should be kept low to inhibit the reverse reaction. Further complication arises from the need to separate oxygen from zinc vapor. The supersaturation of zinc vapor should preferably be high to obtain high deposition rates of zinc, whereas the oxygen should be diluted by the inert gas. The energy storage process results in the agglomeration of zinc atoms forming metal−metal bond clusters.[28]

The zinc oxide formation by reoxidation of zinc was found to be of a heterogeneous nature, with homogeneously condensed zinc serving as the main nucleation sites. The morphology of ZnO particles obtained at low zinc partial pressures show the characteristic tetrapod shape, so-called T-ZnO, with platelets bridging between legs. HRTEM measurements showed that the nucleus has a different crystallographic structure than the leg crystals due to condensed zinc forming at the very initial stage of T-ZnO crystallization. The product inhomogeneity is thus caused by different growth and recombination mechanisms of zinc and zinc oxide.

Unique advantages of a solar furnace are extremely fast heating and cooling rates. Drawbacks are fluctuating power input and temperatures, and shading effects. Keeping isothermal conditions is particularly difficult for the $ZnO/Zn/O_2$ chemical system because of exothermic and endothermic processes occurring during ZnO dissociation, zinc reoxidation, condensation, and evaporation.

By preheating the carrier gas stream it should be possible to avoid the cooling of the products below the condensation temperature of zinc (∼700 °C) before reaching the condenser. The condensation conditions would be better defined.

Keeping a constant zinc partial pressure is also difficult because of the dynamic chemical equilibrium of the experiments.

Acknowledgment. We thank A. Frei and R. Palumbo for their help. This work was enabled through the 1998 scholarship of SOLAR PACES and financial support by the BFE-Swiss Federal Office of Energy.

CM0010295

(28) Weidenkaff, A.; Steinfeld, A.; Wokaun, A.; Reller, A. In *Greenhouse Gas Control Technologies*; Eliason, B., Riemer, P., Wokaun, A., Eds.; Elsevier: Interlaken, 1999.